Human endothelial colony-forming cells serve as trophic mediators for mesenchymal stem cell engraftment via paracrine signaling

Ruei-Zeng Lin[a], Rafael Moreno-Luna[a], Dan Li[b], Shou-Ching Jaminet[b], Arin K. Greene[c], and Juan M. Melero-Martin[a,d,1]

[a]Department of Cardiac Surgery, Boston Children's Hospital, and Department of Surgery, Harvard Medical School, Boston, MA 02115; [b]Center for Vascular Biology, Department of Pathology, Beth Israel Deaconess Medical Center, Boston, MA 02215; [c]Department of Plastic and Oral Surgery, Boston Children's Hospital, Boston, MA 02115; and [d]Harvard Stem Cell Institute, Cambridge, MA 02138

Edited by Robert Langer, Massachusetts Institute of Technology, Cambridge, MA, and approved June 10, 2014 (received for review March 22, 2014)

Endothelial colony-forming cells (ECFCs) are endothelial precursors that circulate in peripheral blood. Studies have demonstrated that human ECFCs have robust vasculogenic properties. However, whether ECFCs can exert trophic functions in support of specific stem cells in vivo remains largely unknown. Here, we sought to determine whether human ECFCs can function as paracrine mediators before the establishment of blood perfusion. We used two xenograft models of human mesenchymal stem cell (MSC) transplantation and studied how the presence of ECFCs modulates MSC engraftment and regenerative capacity in vivo. Human MSCs were isolated from white adipose tissue and bone marrow aspirates and were s.c. implanted into immunodeficient mice in the presence or absence of cord blood-derived ECFCs. MSC engraftment was regulated by ECFC-derived paracrine factors via platelet-derived growth factor BB (PDGF-BB)/platelet-derived growth factor receptor (PDGFR)-β signaling. Cotransplanting ECFCs significantly enhanced MSC engraftment by reducing early apoptosis and preserving stemness-related properties of PDGFR-β$^+$ MSCs, including the ability to repopulate secondary grafts. MSC engraftment was negligible in the absence of ECFCs and completely impaired in the presence of Tyrphostin AG1296, an inhibitor of PDGFR kinase. Additionally, transplanted MSCs displayed fate-restricted potential in vivo, with adipose tissue-derived and bone marrow-derived MSCs contributing exclusive differentiation along adipogenic and osteogenic lineages, respectively. This work demonstrates that blood-derived ECFCs can serve as paracrine mediators and regulate the regenerative potential of MSCs via PDGF-BB/PDGFR-β signaling. Our data suggest the systematic use of ECFCs as a means to improve MSC transplantation.

vasculogenesis | adipogenesis | osteogenesis | angiocrine factors

Endothelial colony-forming cells (ECFCs) are a subset of progenitor cells that circulate in peripheral blood. The identification of ECFCs in humans created a promising opportunity to noninvasively derive large quantities of autologous endothelial cells (ECs) for clinical use (1–3). Indeed, a growing body of preclinical studies has substantiated the therapeutic potential of ECFCs. Initial demonstrations included using ECFCs to endothelialize cardiovascular grafts as a means to achieve effective antithrombogenicity and vascular patency in vivo (4). Studies have also demonstrated that human blood-derived ECFCs have inherent and robust vasculogenic properties. Following transplantation into immunodeficient mice, ECFCs can self-assemble into long-lasting microvascular networks that anastomose with the host vasculature (5, 6). The function of ECFC-lined microvessels has been shown to be similar to that of normal microvessels in several respects, including nonthrombogenicity, blood flow, regulation of macromolecule permeability, and capacity to induce leukocyte-endothelial interactions in response to cytokine activation (5, 7).

Beyond lining cardiovascular structures, ECs regulate multiple physiological processes through the secretion of angiocrine factors (8). During development, the endothelium provides paracrine signals to assist the formation of various organs, including liver and pancreas (9, 10). Emerging evidence indicates that ECs also regulate postnatal homeostatic and regenerative processes via paracrine production of stem cell-active trophic factors (11). For example, signals from bone marrow microvascular ECs are essential for self-renewal and repopulation of hematopoietic stem cells (12). Similarly, EC-derived paracrine signals stimulate self-renewal and in situ expansion of stem cells residing in lung, liver, and neural tissues, contributing to the regeneration of these tissues upon injury (13, 14). Despite this trophic potential, current therapeutic uses of ECFCs remain largely focused on harnessing their inherent blood vessel-forming capacity. However, whether ECFCs can exert trophic functions in support of specific stem cells in vivo is largely unknown.

Here, we investigated whether human cord blood-derived ECFCs can function as paracrine mediators before the establishment of blood perfusion. Toward this aim, we used two preclinical xenograft models of human mesenchymal stem cell (MSC) transplantation and studied how the presence of ECFCs modulates MSC engraftment and regenerative capacity in vivo.

Results

Blood-Derived ECFCs Provide Trophic Support to MSCs Before the Onset of Neovascularization and Blood Perfusion. We examined the paracrine role of ECFCs following s.c. transplantation of human MSCs into immunodeficient mice. We used a model in which both ECFCs and MSCs are embedded as single cells in Matrigel

Significance

Endothelial colony-forming cells (ECFCs) circulate in peripheral blood and contribute to the formation of new vasculature. Here, we demonstrate that ECFCs can also function as paracrine mediators prior to the establishment of blood perfusion, modulating the regenerative potential of human mesenchymal stem cells (MSCs). We show that MSCs are highly dependable on platelet-derived growth factor BB and that ECFCs provide critical angiocrine factors needed to preserve MSCs as viable. This early angiocrine support ultimately enables extensive engraftment and long-term differentiation of transplanted MSCs. This study provides new insights into the biological attributes of ECFCs that may expand their therapeutic potential. We foresee the use of ECFCs as a means to improve the outcome of MSC transplantation.

Author contributions: R.-Z.L. and J.M.M.-M. designed research; R.-Z.L., R.M.-L., and D.L. performed research; S.-C.J. and A.K.G. contributed new reagents/analytic tools; R.-Z.L., R.M.-L., D.L., S.-C.J., A.K.G., and J.M.M.-M. analyzed data; and R.-Z.L. and J.M.M.-M. wrote the paper.

The authors declare no conflict of interest.

This article is a PNAS Direct Submission.

[1]To whom correspondence should be addressed. E-mail: juan.meleromartin@childrens.harvard.edu.

This article contains supporting information online at www.pnas.org/lookup/suppl/doi:10.1073/pnas.1405388111/-/DCSupplemental.

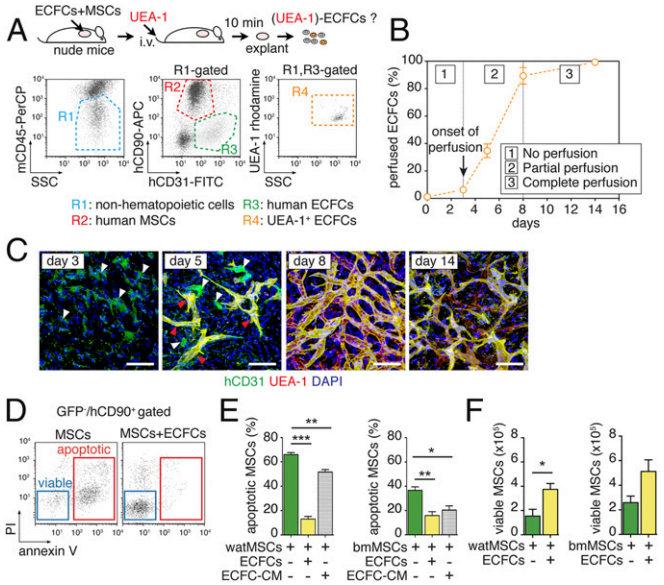

Fig. 1. ECFCs provide trophic support to MSCs before the onset of perfusion. (*A*) Human ECFCs and MSCs were transplanted into nude mice. Rhodamine-conjugated UEA-1 was i.v.-injected into implant-bearing mice 10 min before harvesting the implants. Retrieved cells were identified by flow cytometry as follows: nonhematopoietic cells (mCD45$^-$ cells; R1 gate); human MSCs (mCD45$^-$/hCD90$^+$/hCD31$^-$ cells; R2 gate); total human ECFCs (mCD45$^-$/hCD90$^-$/hCD31$^+$ cells; R3 gate); and perfused (UEA-1$^+$) ECFCs (mCD45$^-$/hCD90$^-$/hCD31$^+$/UEA-1$^+$ cells; R4 gate). (*B*) Cytometric quantification of perfused human ECFCs in explanted grafts. (*C*) Projections of whole-mount fluorescent staining of explanted grafts. ECFCs were identified by expression of hCD31 (green) and perfused ECFCs by UEA-1 (red). (Scale bars, 100 μm.) (*D*) MSCs were implanted into GFP-SCID mice with or without ECFCs. Viable (PI$^-$/annexin-V$^-$) and apoptotic (annexin-V$^+$) MSCs were identified at day 2 by flow cytometry. (*E*) Percentage of apoptotic MSCs at day 2 in grafts with or without ECFCs and ECFC-CM. (*F*) Number of viable MSCs at day 7 in grafts with or without ECFCs. Bars represent mean ± SEM. Mice per group: $n = 4$. $^*P < 0.05$, $^{**}P < 0.01$, and $^{***}P < 0.001$ compared with grafts with MSCs alone.

(Fig. 1*A*). ECFCs progressively assembled into functional capillaries in vivo. The percentage of ECFCs that formed part of perfused vessels was determined at time intervals following i.v. infusion of rhodamine-conjugated UEA-1 lectin (hCD31$^+$/UEA-1$^+$ cells in Fig. 1 *A*–*C*). There were three distinct phases with regards to ECFC contribution into perfused vascular structures: (*i*) an initial 3-d lag phase where most ECFCs were still not part of a perfused blood vessel (>93% ECFCs were UEA-1$^-$ at day 3; Fig. 1*B*); (*ii*) a transitional phase between days 3 and 8 where ECFCs rapidly incorporated into perfused vasculature; and (*iii*) a phase of complete perfusion (>99% UEA-1$^+$ ECFCs by day 14; Fig. 1*B*). Thus, day 3 was identified as the onset of perfusion (Fig. 1*B*). Before this onset, ECFCs were uniformly distributed throughout the implants but not as part of perfused lumens (Fig. 1*C*).

To study flow-independent cellular functions, we cotransplanted ECFCs with MSCs and examined the grafts during the initial perfusion-free period. We studied the effect of ECFCs on two distinct human MSCs obtained from the stromal vascular fraction of normal white adipose tissue (watMSCs) and bone marrow aspirates (bmMSCs). Both watMSCs and bmMSCs were isolated based on their colony-forming unit–fibroblast (CFU-F) activity (*SI Appendix*, Fig. S1), and their phenotype and purity were extensively characterized before implantation (*SI Appendix*, Figs. S1 and S2). Also, both watMSCs and bmMSCs had a similar capacity to support vasculogenesis in vivo (*SI Appendix*, Fig. S3). Examination of cells in the grafts at day 2 revealed a marked lost of MSC viability in the absence of ECFCs, a process that occurred via cell apoptosis (Fig. 1*D*). The prevention of MSC apoptosis by ECFCs suggested a trophic support that preceded the onset of neovascularization. Indeed, at day 2, only 13 ± 2% of all watMSCs were apoptotic when cotransplanted with ECFCs, as opposed to 66 ± 2% in single-cell grafts (Fig. 1*E*). Similarly, bmMSC apoptosis was reduced from 37 ± 3% to 16 ± 3% in the presence of ECFCs (Fig. 1*E*). Moreover, this trophic function was mediated by ECFC-derived paracrine factors; providing ECFC-conditioned media (ECFC-CM) in implants without ECFCs significantly reduced apoptosis of both watMSCs and bmMSCs (Fig. 1*E*). As expected, the early prevention of MSC apoptosis by ECFCs produced a significant increase in the number of viable MSCs that were effectively available at day 7 in already perfused grafts (Fig. 1*F*; *SI Appendix*, Fig. S4).

Loss of MSC Regenerative Capacity in the Absence of Early Angiocrine Support. To gain further insights into the trophic support provided by ECFCs, we evaluated whether MSCs had undergone functional changes following transplantation. To this aim, MSCs were implanted with or without ECFCs into GFP-SCID mice. MSCs were then retrieved at day 7 and purified by virtue of hCD90 expression (Fig. 2*A*; *SI Appendix*, Fig. S5). We observed that the CFU-F activity of MSCs was better preserved in the presence of ECFCs (Fig. 2 *B* and *C*). Indeed, watMSCs retrieved at day 7 from implants coseeded with ECFCs maintained significantly more CFU-F activity (42 ± 3 colonies) than those from implants without ECFCs (13 ± 2 colonies) (Fig. 2*C*). Similar results were found on retrieved bmMSCs (42 ± 9 colonies with ECFCs versus 12 ± 5 colonies without ECFCs; Fig. 2*C*). Of note, we ensured that we enumerated only colonies with CFU-F activity that originated from retrieved human MSCs and thus lacked both GFP expression and UEA-1–binding affinity (*SI Appendix*, Fig. S6). In addition, cotransplanting ECFCs altered the ex vivo differentiation potential of retrieved MSCs. The percentage of randomly selected clones that retained adipogenic, osteogenic, and double differentiation potential decreased when the parental MSCs were derived from implants without ECFCs, an observation that was valid for both watMSCs and bmMSCs (Fig. 2 *D* and *E*). Taken together, the trophic support provided by ECFCs not only improved short-term MSC engraftment, but also helped to preserve the clonogenic and differentiation potential of the transplanted MSCs.

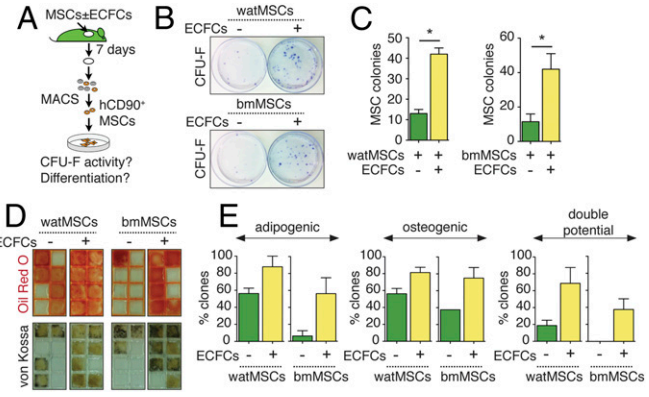

Fig. 2. Loss of MSC properties in the absence of early angiocrine support. (*A*) MSCs were transplanted into GFP-SCID mice with or without ECFCs and then retrieved at day 7 and selected as hCD90$^+$ cells ($n = 3$ per group). (*B*) Enhanced CFU-F activity in MSCs from ECFC-containing grafts (5×10^2 MSCs plated per group). (*C*) Quantitative CFU-F activity of retrieved MSCs. (*D*) Ex vivo adipogenic and osteogenic differentiation of retrieved MSCs at clonal density ($n = 16$ clones per group). (*E*) Percentage of MSC clones with single and double differentiation potential after retrieval from grafts. Bars represent mean ± SEM. $^*P < 0.05$ compared with grafts with MSCs alone.

Next, we examined the in vivo regenerative capacity of MSCs. First, we studied long-term adipogenic engraftment of watMSCs using a xenograft model of s.c. transplantation into immunodeficient mice. Histological examinations of explanted grafts revealed a marked difference in adipocyte content depending on whether ECFCs were cotransplanted with MSCs (Fig. 3*A*). After 28 d, adipocyte density in implants seeded with watMSCs+ECFCs (418 ± 45 adipocytes/mm^2) was significantly higher than in grafts with only watMSCs (19 ± 6 adipocytes/mm^2) (Fig. 3*C*). The effect of ECFCs on adipocyte density was observed in both Matrigel (Fig. 3) and collagen/fibronectin hydrogels (*SI Appendix*, Fig. S7). In addition, watMSC-derived adipocytes were highly similar in size to native adipocytes (Fig. 3*D*), which indicated mature differentiation. Perilipin-A$^+$ adipocytes that originated from donor MSCs were identified by virtue of human vimentin expression (h-vimentin; Fig. 3*B*; see *SI Appendix*, Fig. S8 for antibody specificity). At day 28, grafts were completely surrounded by host s.c. adipose tissue (perilipin-A$^+$/h-vimentin$^-$; Fig. 3*B*); however, the adipocytes found inside watMSCs+ECFCs implants originated mostly from donor human MSCs (92 ± 4%; Fig. 3*E*). In contrast, the donor MSC contribution to adipocytes was significantly reduced in grafts without ECFCs (12 ± 3%; Fig. 3*E*). This ECFC support to MSC engraftment was confirmed in GFP-SCID mice, where the relative contribution of host and donor cells was elucidated by virtue of GFP expression (*SI Appendix*, Fig. S9). In addition, we corroborated the changes in differentiation potential by transplanting retrieved MSCs into secondary mice (Fig. 3*F*). Only watMSCs that had been primarily transplanted with ECFCs were able to differentiate along the adipogenic lineage (h-vimentin$^+$/perilipin-A$^+$ cells) in secondary grafts (Fig. 3*F*).

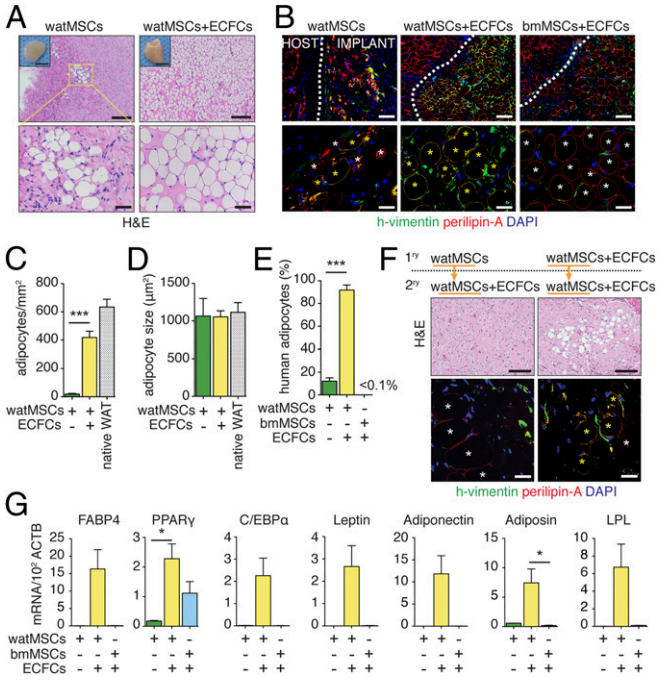

Fig. 3. Irreversible loss of watMSC adipogenic potential in the absence of initial angiocrine support. (*A*) MSCs were transplanted into nude mice with or without ECFCs for 28 d, and H&E staining of grafts was performed. (*Insets*) Macroscopic explants. (*B*) Immunohistochemical analysis of adipocytes in explanted grafts. Adipocytes express perilipin-A (red). Human MSC-derived cells express h-vimentin (green). Yellow asterisks: human adipocytes. White asterisks: murine adipocytes. (*C*) Quantification of adipocyte density. (*D*) Adipocyte size in explants. (*E*) Percentage of human adipocytes (perilipin-A$^+$/h-vimentin$^+$). (*F*) watMSCs were transplanted into primary GFP-SCID mice for 7 d and then retrieved and transplanted with ECFCs into secondary nude mice for 28 d. H&E and immunofluorescence staining was used for secondary grafts. Yellow asterisks: human adipocytes. White asterisks: murine adipocytes. (*G*) mRNA expression of adipogenic factors in explanted grafts. All primers were human-specific (*SI Appendix*, Table S1). Data are normalized to human β-actin (*ACTB*). [Scale bars: 200 μm (*A*, *B*, and *F*, *Upper*); 50 μm (*A*, *B*, and *F*, *Lower*); and 5 mm (*A*, *Insets*).] Bars represent mean ± SEM ($n = 4$ mice per group). *$P < 0.05$. ***$P < 0.001$ compared with grafts with MSCs alone.

Implants seeded with bmMSCs+ECFCs also had numerous adipocytes at day 28 (Fig. 3*B*). However, unlike with watMSCs, adipocytes were entirely of murine origin (h-vimentin$^-$/perilipin-A$^+$) (Fig. 3*E*), indicating that in vivo adipogenic differentiation potential was restricted to adipose tissue-derived MSCs. Differentiation along adipogenic lineage was also confirmed at the mRNA level by expression of adipose-specific hormones, adipokines, and transcription factors. Implants seeded with watMSCs+ECFCs expressed human-specific *FABP4*, *PPARγ*, *C/EBPα*, *leptin*, *adiponectin*, *adiposin*, and *LPL* at higher levels than in grafts seeded with either watMSCs alone or with bmMSCs+ECFCs (Fig. 3*G*). This presence of adipose-specific factors in watMSCs+ECFCs grafts was indicative of adequate human adipocyte function at day 28.

Next, we studied the effect of ECFCs on bmMSC engraftment and osteogenic differentiation using an ectopic BMP-2–induced s.c. model. Histological examinations of von Kossa-stained sections from grafts revealed marked differences in the extent of tissue mineralization achieved with or without ECFCs (Fig. 4*A*). At 28 d, the percentage of mineralized area in implants seeded with bmMSCs+ECFCs (2.9 ± 1.9%) was significantly higher than in implants with only bmMSCs (0.1 ± 0.1%). Of note, unlike other reports that used stiffer polymeric scaffolds (15), mineralization inside Matrigel was completely dependable on the provision of BMP-2 (Fig. 4*C*). BMP-2–stimulated grafts had numerous osterix$^+$ osteoblasts distributed throughout the implant (Fig. 4*B*). Most osteoblasts found inside implants seeded with bmMSCs+ECFCs originated from donor human MSCs (osterix$^+$/h-vimentin$^+$ cells; 62 ± 9%; Fig. 4*D*). In contrast, differentiation of donor MSCs into osteoblasts was significantly reduced without ECFCs (8 ± 2%; Fig. 4*D*). Grafts seeded with watMSCs+ECFCs also had numerous osterix$^+$ osteoblasts at day 28 (Fig. 4*B*). However, unlike with bmMSCs, osteoblasts were entirely of murine origin (h-vimentin$^-$/osterix$^+$) and did not originate from donor watMSCs, indicating fate-restricted potential. Moreover, only bmMSCs that had been transplanted with ECFCs in primary mice were able to differentiate into human osteoblasts (h-vimentin$^+$/osterix$^+$ cells) upon transplantation into secondary mice (Fig. 4*E*). In contrast, bmMSCs that were primarily transplanted without ECFCs had completely lost their capacity to differentiate in secondary grafts (Fig. 4*E*). At the mRNA level, expression of human-specific *RUNX2*, *SOX9*, and *osterix* was higher in grafts seeded with bmMSCs+ECFCs than in those with either bmMSCs alone or with watMSCs+ECFCs (Fig. 4*F*). Additionally, implants seeded with bmMSCs, but not watMSCs, expressed high levels of human *osteopontin* and *osteocalcin* (Fig. 4*F*), indicating ongoing mineralization by human osteoblasts.

Taken together, we demonstrated that before the onset of vascularization the absence of early angiocrine support compromised the regenerative capacity of both watMSCs and bmMSCs.

Endothelial Modulation of MSC Regenerative Capacity Is Driven by Paracrine Platelet-Derived Growth Factor BB Signaling. To elucidate which angiocrine signals were involved in supporting MSC engraftment, we first identified ECFC-derived factors that were secreted only by ECFCs and not by MSCs, including endothelin 1 (ET-1), platelet-derived growth factor (PDGF)-AA, EGF, PDGF-BB, heparin binding-EGF, and basic fibroblast growth factor (angiocrine factors; Fig. 5*A*). Among these candidates, we focused on PDGF-BB because this angiocrine factor was consistently absent in ECFC-MSC cocultures, suggesting preferential

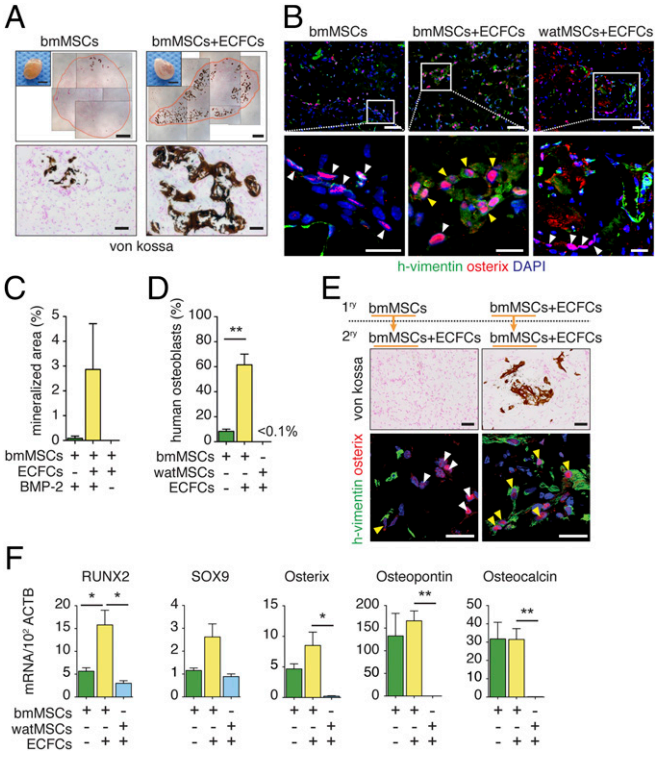

Fig. 4. Irreversible loss of bmMSC osteogenic potential in the absence of initial angiocrine support. (*A*) MSCs were implanted into nude mice with or without ECFCs and BMP-2 for 28 d. von Kossa staining was used for the grafts. Top panels are montages of contiguous pictures capturing the entire cross-section of the explants, with dashed black lines delineating the border of each mounted picture. (*Insets*) Macroscopic views of the explants. (*B*) Immunohistochemical analysis of osteogenic differentiation. Osteoblasts express osterix (red). Human MSC-derived cells express h-vimentin (green). Yellow arrowheads: human osteoblasts. White arrowheads: murine osteoblasts. (*C*) Quantification of tissue mineralization. (*D*) Percentage of human osteoblasts (osterix$^+$/h-vimentin$^+$). (*E*) bmMSCs were transplanted into primary GFP-SCID mice for 7 d and then retrieved and transplanted with ECFCs into secondary nude mice for 28 d. von Kossa and immunofluorescence staining was used for BMP-2–stimulated secondary grafts. Yellow arrowheads: human osteoblasts. White arrowheads: murine osteoblasts. (*F*) mRNA expression of osteogenic factors. All primers were human-specific (*SI Appendix*, Table S1). Data are normalized to human β-actin (*ACTB*). [Scale bars: 1 mm (*A*, *Upper*); 200 μm (*A*, *Lower*; *E*, *Upper*); 3 mm (*A*, *Insets*); 50 μm (*B*, *Upper*); and 10 μm (*B* and *E*, *Lower*).] Bars represent mean ± SEM ($n = 4$ mice per group). *$P < 0.05$. **$P < 0.01$ compared with grafts with MSCs alone.

utilization by MSCs (Fig. 5*B*). Also, transcriptional expression of *PDGF-B* was restricted to ECFCs, whereas its receptor [platelet-derived growth factor receptor (*PDGFR*)-*β*] was preferentially expressed by MSCs (Fig. 5*C*). Indeed, ECFCs expressed *PDGF-B* constitutively both in vitro and in vivo (*SI Appendix*, Fig. S10). Adding PDGF-BB (100 ng) to our grafts significantly increased the number of viable MSCs at day 2, even in the absence of ECFCs (Fig. 5*D*). Also, the in vivo trophic support provided by ECFCs was effectively neutralized with Tyrphostin AG1296, an inhibitor of PDGFR kinase (Fig. 5*D*). Moreover, blocking PDGF-BB/PDGFR-β signaling in grafts containing ECFCs altered the clonogenic and differentiation potential of transplanted MSCs (*SI Appendix*, Fig. S11), even though AG1296 did not interfere with the vascularization of the grafts in vivo (*SI Appendix*, Fig. S12) and did not induce apoptosis nor impair the differentiation potential of MSCs in vitro (*SI Appendix*, Fig. S13). Notably, blocking PDGF-BB/PDGFR-β signaling (via one single dose of AG1296) completely abrogated the long-term regenerative capacity of MSCs. Subcutaneous implants containing watMSCs+ECFCs and treated with AG1296 at the time of implantation had no detectable human perilipin-A$^+$ adipocytes by day 28 (Fig. 5*E*). Additionally, silencing PDGF-B expression in ECFCs via siRNA produced a partial reduction in the number of viable watMSCs present in the grafts at day 2 (*SI Appendix*, Fig. S14). Similarly, provision of AG1296 impaired BMP-2–driven differentiation of bmMSCs along the osteogenic lineage, with no detectable human osterix$^+$ osteoblasts by day 28 (Fig. 5*F*). Finally, despite the fact that provision of PDGF-BB enhanced short-term MSC survival in the absence of ECFCs (Fig. 5*D*), this factor alone did not permit long-term differentiation of transplanted MSCs (*SI Appendix*, Fig. S15), indicating that a single dose of 100 ng of PDGF-BB was insufficient to replace the full trophic potential of ECFCs.

To further elucidate the role of PDGF-BB, we examined the spatial distribution of PDGFR-β expression on transplanted MSCs. MSCs occupied both perivascular (h-vimentin$^+$/α-SMA$^+$) and interstitial (h-vimentin$^+$/α-SMA$^-$) locations within the implants (*SI Appendix*, Fig. S16). However, the perivascular contribution was significantly more abundant when MSCs were cotransplanted

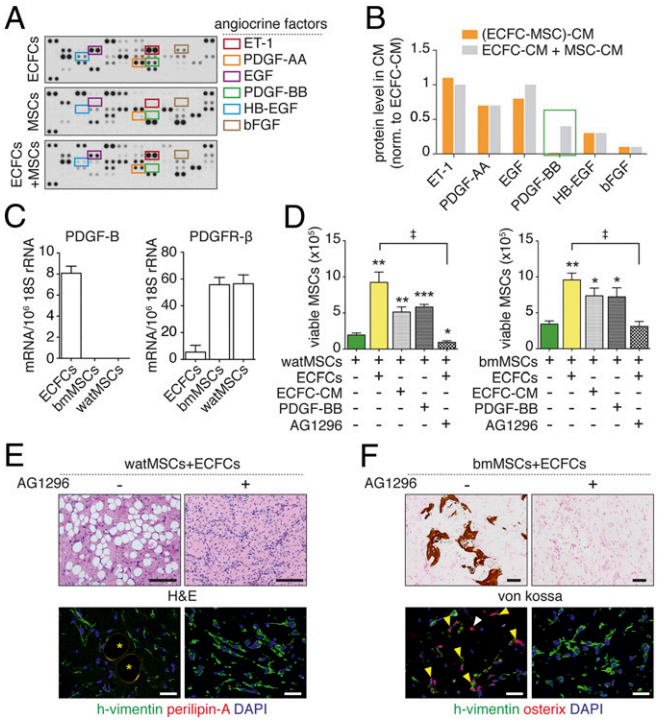

Fig. 5. ECFCs support MSC engraftment via paracrine secretion of PDGF-BB. (*A*) Protein arrays of conditioned media from ECFCs, MSCs, and MSCs+ECFCs (1:1 ratio). Color-lined boxes indicate ECFC-secreted angiocrine factors. (*B*) Quantification of angiocrine factors: (*i*) conditioned medium from ECFC-MSC coculture [(ECFC-MSC)-CM]; (*ii*) A 1:1 mixture of conditioned media from monocultures of ECFCs and MSCs (ECFC-CM+MSC-CM). (*C*) mRNA expression of PDGF-B and PDGFR-β in ECFCs, watMSCs, and bmMSCs. Data normalized to ribosomal 18S rRNA. (*D*) Flow cytometry quantification of viable MSCs at day 2 in grafts with or without ECFCs, ECFC-CM, PDGF-BB, and PDGFR inhibitor (AG1296). (*E*) MSCs were transplanted into nude mice with ECFCs with or without AG1296. H&E and immunofluorescence staining were performed at day 28. Human adipocytes: perilipin-A$^+$/h-vimentin$^+$ cells (yellow asterisks). (*F*) MSCs were transplanted into nude mice with ECFCs, BMP-2, and with or without AG1296. von Kossa and immunofluorescence staining were performed at day 28. Human osteoblasts: osterix$^+$/h-vimentin$^+$ cells (yellow arrowheads). [Scale bars: 200 μm (*E* and *F*, *Upper*) and 50 μm (*E* and *F*, *Lower*).] Bars represent mean ± SEM ($n = 4$ mice per group). *$P < 0.05$, **$P < 0.01$, and ***$P < 0.001$ compared with grafts with MSCs alone. ‡$P < 0.01$ compared with grafts with MSCs+ECFCs.

with ECFCs (*SI Appendix*, Fig. S16). This dual MSC localization coincided with a differential expression of perivascular markers, including PDGFR-β (Fig. 6 *A* and *B*). After 7 d in vivo, 43 ± 12% of MSCs that were coseeded with ECFCs expressed PDGFR-β (Fig. 6*B*). In contrast, both the absence of ECFCs and the inhibition of PDGFR signaling significantly reduced the percentage of PDGFR-β$^+$ MSCs (17 ± 3% and 19 ± 3%, respectively; Fig. 6*B*). We also examined phenotypical and functional differences between perivascular and interstitial MSCs in vivo. To this aim, we obtained watMSCs from grafts that were implanted into GFP-SCID mice for 7 d. Retrieved watMSCs were then FACS-sorted into (*i*) GFP$^-$/hCD90$^+$/PDGFR-β$^+$ cells (referred to as PDGFR-β$^+$ watMSCs) and (*ii*) GFP$^-$/hCD90$^+$/PDGFR-β$^-$ cells (PDGFR-β$^-$ watMSCs) (Fig. 6*C*). Of note, PDGFR-β$^-$ watMSCs acquired expression of PDGFR-β in culture (*SI Appendix*, Fig. S17), and thus it is important to separate PDGFR-β$^+$/PDGFR-β$^-$ cells immediately after retrieval. Quantitative RT-PCR analyses carried out in noncultured cells confirmed the perivascular/interstitial dichotomy of the sorted MSCs. Hierarchical clustering revealed that PDGFR-β$^+$ watMSCs were similar to human smooth muscle cells (SMCs) and expressed high levels of the perivascular markers *PDGFR-β*, *SM22*, *α-SMA*, and *MYH11* (Fig. 6*D*). Meanwhile, the transcriptional profile of PDGFR-β$^-$ watMSCs resembled that of normal human dermal fibroblasts (NHDFs), including higher expression of *PDGFR-α*, *desmin*, and *Ang1* (Fig. 6*D*). Importantly, perivascular PDGFR-β$^+$ watMSCs retained CFU-F activity (Fig. 6*E*) and differentiation potential (Fig. 6 *F* and *G*) that was superior to PDGFR-β$^-$ watMSCs. The loss of stem cell properties in PDGFR-β$^-$ watMSCs occurred despite the fact that these cells acquired PDGFR-β expression in culture, indicating that in vitro PDGFR-β expression per se is not reflective of stemness. Indeed, only PDGFR-β$^+$ watMSCs were able to differentiate along the adipogenic lineage (h-vimentin$^+$/perilipin-A$^+$ cells) upon transplantation into secondary mice. In contrast, PDGFR-β$^-$ watMSCs derived from primary implants had completely lost their capacity to differentiate into human adipocytes in secondary grafts (Fig. 6*G*).

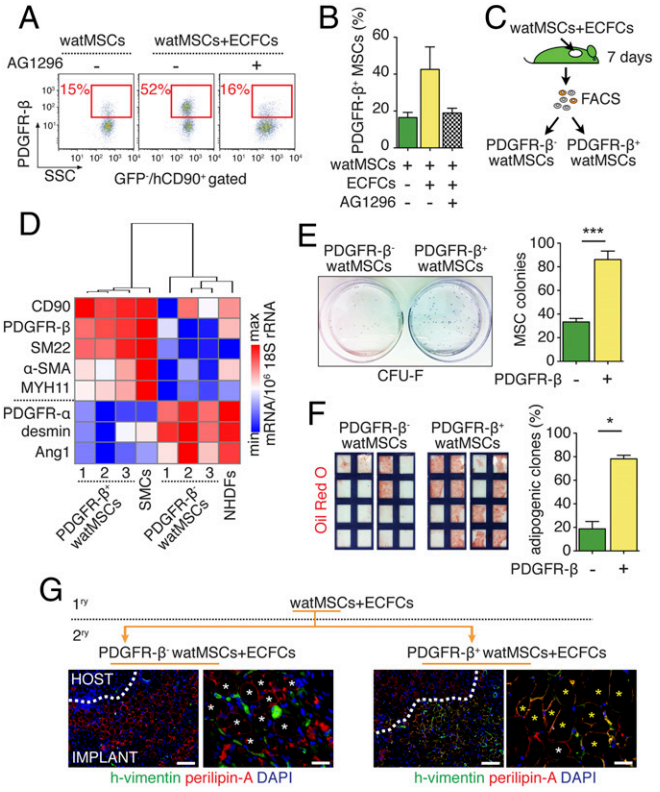

Fig. 6. PDGFR-β expression in transplanted MSCs coincides with progenitor cell function. (*A*) Flow cytometric detection of PDGFR-β$^+$ watMSCs in grafts with or without ECFCs and PDGFR inhibitor (AG1296). (*B*) Percentage of PDGFR-β$^+$ watMSCs at day 7. (*C*) watMSCs were transplanted into GFP-SCID mice with ECFCs, retrieved at day 7, and immediately sorted into PDGFR-β$^+$ and PDGFR-β$^-$ cells. (*D*) Heat map and hierarchical clustering of sorted watMSCs. mRNA data are normalized to ribosomal 18S rRNA. Human SMCs and NHDFs served as controls. (*E*) CFU-F activity of sorted watMSCs. (*F*) Ex vivo adipogenic differentiation potential of sorted watMSCs. (*G*) watMSCs were transplanted into primary mice with ECFCs. Retrieved watMSCs (day 7) were sorted into PDGFR-β$^+$ and PDGFR-β$^-$ cells and separately transplanted with ECFCs into secondary mice for 28 d. Immunofluorescence staining of secondary grafts was performed. Yellow asterisks: human adipocytes (perilipin-A$^+$/h-vimentin$^+$). White asterisks: murine adipocytes (perilipin-A$^+$/h-vimentin$^-$). [Scale bars: 200 μm (*G*, *Left* panels) and 50 μm (*G*, *Right* panels).] Bars represent mean ± SEM. Mice per group: $n = 4$ (*B*), $n = 3$ (*D*–*G*). Clones per group: $n = 16$ (*F*). $^*P < 0.05$; $^{***}P < 0.001$.

Discussion

In the present study, we used xenograft models of human cell transplantation to demonstrate that blood-derived ECFCs can function as paracrine mediators before the establishment of perfusion, modulating the regenerative potential of MSCs. We showed that ECFC trophic support of MSCs was driven by PDGF-BB/PDGFR-β signaling. PDGFR-β$^+$ MSCs were highly dependable on PDGF-BB, and they preferentially resided in perivascular locations within the vascularized implants. Importantly, before the onset of vascularization and perfusion, cotransplanted ECFCs provided critical angiocrine factors needed to preserve PDGFR-β$^+$ MSC viability. This early angiocrine support ultimately enabled extensive engraftment and long-term lineage-restricted differentiation of transplanted MSCs.

Heterotypic interactions between ECs and MSCs are crucial in vascular development, and PDGF signaling is particularly critical as it regulates the perivascular recruitment of MSCs (16). Indeed, both PDGFR-β and PDGF-BB ligand-null mice die prenatally from hemorrhage and lack pericytes throughout the entire microvascular beds (17, 18). Postnatally, mounting evidence indicates that paracrine signals between ECs and MSCs are also essential for the proper functioning of various stem cell niches (19, 20). In fact, the distribution of MSCs within postnatal tissues is related to their existence in vascular niches (21). In culture, however, isolated MSCs are separated from ECs, and thus crosstalk between these two cell types is lost. Here, we demonstrated that rapidly restoring this heterotypic cellular interaction in vivo is crucial for proper MSC function. In our models of cell transplantation, short-term absence of angiocrine support produced an irreversible loss of regenerative potential in MSCs. Following cotransplantation with ECFCs, MSCs spontaneously dichotomized into PDGFR-β$^+$ and PDGFR-β$^-$ cells, acquiring distinct perivascular and interstitial cell phenotypes, respectively. Between these two subpopulations, only PDGFR-β$^+$ MSCs retained robust regenerative potential and were able to repopulate grafts in secondary animals. However, in the absence of early angiocrine support, the majority of PDGFR-β$^+$ MSCs underwent apoptosis soon after transplantation, leading to grafts with no differentiated donor cell contribution. Blocking PDGF signaling produced a similar effect. Hence, our study underscores the importance of maintaining MSC–EC proximity. Cotransplanting ECFCs in conjunction with MSCs was proven an effective means to prevent premature apoptosis of PDGFR-β$^+$ MSCs. An alternative to the provision of ECFCs would be to attain EC-derived trophic factors via recruitment of host ECs. However, we showed that apoptosis of PDGFR-β$^+$ MSCs preceded the infiltration of host vasculature into the implants, and thus the initial provision of ECFCs was indeed critical. Also, although simply adding exogenous PDGF-BB reduces MSC apoptosis, unregulated provision of PDGF-BB in vivo could be

detrimental and produce vascular regression (22). This regression does not occur with ECFCs, which can modulate in a timely way the delivery of PDGF-BB and other paracrine factors during their interaction with MSCs.

From a translational standpoint, our results suggest the use of ECFCs as a means to improve the outcome of MSC transplantation. Currently, there are hundreds of MSC-based clinical trials registered at https://clinicaltrials.gov targeting a plethora of conditions, including cardiovascular diseases and immune-mediated disorders. However, none of these clinical trials incorporate ECs as therapeutic agents because most investigators have resisted using two or more different cell types, which increases the complexity of phase I studies exponentially. The reality is, however, that despite tremendous advance in our knowledge of human MSC biology, conclusive evidence of any therapeutic efficacy of MSCs remains elusive and continues to be debated (23, 24). The lack of efficacy has been attributed to multiple factors, including insufficient understanding of pharmacokinetics of the administered cells. Numerous preclinical studies have shown that i.v.-infused MSCs primarily embolize in the lungs and other nontarget organs (25, 26). Nevertheless, most trials continue to infuse MSCs systemically, which likely produces insufficient cell engraftment at target sites. Whether MSCs can promote tissue repair without targeted engraftment, via secretion of trophic factors, remains a subject of investigation (27). However, whatever effects embolized MSCs may exert on distant tissues appear to be short-lived and directed to exploit nonprogenitor MSC functions. Certainly, controlling engraftment and differentiation of locally transplanted MSCs remains a major challenge (23). Here, we reason that the lack of appropriate MSC–EC interaction could explain the low engraftment efficacy observed in single-cell transplantation models as well as in clinical trials. In our xenograft models, we demonstrated that a transient lack of EC proximity is sufficient to impair the progenitor function of transplanted MSCs, compromising their long-term regenerative capacity. We found that simply cotransplanting ECFCs into the grafts provides sufficient trophic support to MSCs before the onset of perfusion and via secretion of angiocrine factors, including PDGF-BB.

Finally, the ubiquity and multilineage differentiation potential of MSCs have been intensively debated in recent years. Human MSCs are ubiquitous and reside in a broad range of tissues as perivascular cells, including the bone marrow, adipose tissue, and skeletal muscle (21). Ex vivo, under controlled culture conditions, most perivascular MSCs display multilineage differentiation potential, independently of their anatomical origin (28). However, in vivo studies have often indicated a more lineage-restricted potential. Thus, whether MSCs possess multilineage potential in vivo remains unclear. Our data indicate that multipotency ex vivo does not reflect how MSCs will function in vivo and that transplanted MSCs display linage-restricted potential that is related to their tissue of origin. For example, despite the fact that both watMSCs and bmMSCs displayed multipotency ex vivo, only watMSCs contributed substantial differentiation along adipogenic lineage in vivo. Similarly, bmMSCs, but not watMSCs, contributed ectopic differentiation along osteogenic lineage. Importantly, both watMSCs and bmMSCs had a similar capacity to support vasculogenesis in vivo, and thus the fate-restricted characteristics of these cells were not attributable to differences in vascularization potential. Further studies should identify the mechanisms that regulate fate restriction in human MSCs as well as strategies to reeducate MSCs and enable their differentiation along desired lineages. Certainly, additional insights into the biological attributes of MSCs should result in a more rational exploitation of their therapeutic potential. In light of our results, we propose the systematic use of ECFCs as a means to support MSC engraftment. Whether and how signals from ECFCs influence the fate-restricted characteristics of MSCs remains to be investigated.

Materials and Methods

Animal experiments were conducted under a protocol approved by the Institutional Animal Care and Use Committee at Boston Children's Hospital. Human normal discarded subcutaneous white adipose tissues were obtained in accordance with an Institutional Review Board-approved protocol. Experimental methods are described in detail in *SI Appendix*.

ACKNOWLEDGMENTS. We thank Dr. Reid A. Maclellan, Matthew Vivero, and Javier Couto (Department of Plastic and Oral Surgery, Boston Children's Hospital) for facilitating acquisition of discarded human adipose tissue and Dr. Andrew C. Dudley (University of North Carolina at Chapel Hill) for kindly providing GFP transgenic SCID mice. This work was supported by National Institutes of Health Grant R00EB009096 (to J.M.M.-M.).

1. Lin Y, Weisdorf DJ, Solovey A, Hebbel RP (2000) Origins of circulating endothelial cells and endothelial outgrowth from blood. *J Clin Invest* 105(1):71–77.
2. Ingram DA, et al. (2004) Identification of a novel hierarchy of endothelial progenitor cells using human peripheral and umbilical cord blood. *Blood* 104(9):2752–2760.
3. Melero-Martin JM, et al. (2007) In vivo vasculogenic potential of human blood-derived endothelial progenitor cells. *Blood* 109(11):4761–4768.
4. Kaushal S, et al. (2001) Functional small-diameter neovessels created using endothelial progenitor cells expanded ex vivo. *Nat Med* 7(9):1035–1040.
5. Melero-Martin JM, et al. (2008) Engineering robust and functional vascular networks in vivo with human adult and cord blood-derived progenitor cells. *Circ Res* 103(2):194–202.
6. Traktuev DO, et al. (2009) Robust functional vascular network formation in vivo by cooperation of adipose progenitor and endothelial cells. *Circ Res* 104(12):1410–1420.
7. Au P, et al. (2008) Differential in vivo potential of endothelial progenitor cells from human umbilical cord blood and adult peripheral blood to form functional long-lasting vessels. *Blood* 111(3):1302–1305.
8. Cleaver O, Melton DA (2003) Endothelial signaling during development. *Nat Med* 9(6):661–668.
9. Lammert E, Cleaver O, Melton D (2001) Induction of pancreatic differentiation by signals from blood vessels. *Science* 294(5542):564–567.
10. Matsumoto K, Yoshitomi H, Rossant J, Zaret KS (2001) Liver organogenesis promoted by endothelial cells prior to vascular function. *Science* 294(5542):559–563.
11. Nolan DJ, et al. (2013) Molecular signatures of tissue-specific microvascular endothelial cell heterogeneity in organ maintenance and regeneration. *Dev Cell* 26(2):204–219.
12. Butler JM, et al. (2010) Endothelial cells are essential for the self-renewal and repopulation of Notch-dependent hematopoietic stem cells. *Cell Stem Cell* 6(3):251–264.
13. Shen Q, et al. (2004) Endothelial cells stimulate self-renewal and expand neurogenesis of neural stem cells. *Science* 304(5675):1338–1340.
14. Lee J-H, et al. (2014) Lung stem cell differentiation in mice directed by endothelial cells via a BMP4-NFATc1-thrombospondin-1 axis. *Cell* 156(3):440–455.
15. Kaigler D, et al. (2005) Endothelial cell modulation of bone marrow stromal cell osteogenic potential. *FASEB J* 19(6):665–667.
16. Folkman J, D'Amore PA (1996) Blood vessel formation: What is its molecular basis? *Cell* 87(7):1153–1155.
17. Lindahl P, Johansson BR, Levéen P, Betsholtz C (1997) Pericyte loss and microaneurysm formation in PDGF-B-deficient mice. *Science* 277(5323):242–245.
18. Soriano P (1994) Abnormal kidney development and hematological disorders in PDGF beta-receptor mutant mice. *Genes Dev* 8(16):1888–1896.
19. Greenbaum A, et al. (2013) CXCL12 in early mesenchymal progenitors is required for haematopoietic stem-cell maintenance. *Nature* 495(7440):227–230.
20. Kunisaki Y, et al. (2013) Arteriolar niches maintain haematopoietic stem cell quiescence. *Nature* 502(7473):637–643.
21. Crisan M, et al. (2008) A perivascular origin for mesenchymal stem cells in multiple human organs. *Cell Stem Cell* 3(3):301–313.
22. Au P, et al. (2009) Paradoxical effects of PDGF-BB overexpression in endothelial cells on engineered blood vessels in vivo. *Am J Pathol* 175(1):294–302.
23. Bianco P, et al. (2013) The meaning, the sense and the significance: Translating the science of mesenchymal stem cells into medicine. *Nat Med* 19(1):35–42.
24. Nombela-Arrieta C, Ritz J, Silberstein LE (2011) The elusive nature and function of mesenchymal stem cells. *Nat Rev Mol Cell Biol* 12(2):126–131.
25. Barbash IM, et al. (2003) Systemic delivery of bone marrow-derived mesenchymal stem cells to the infarcted myocardium: Feasibility, cell migration, and body distribution. *Circulation* 108(7):863–868.
26. Lee R-H, et al. (2009) Intravenous hMSCs improve myocardial infarction in mice because cells embolized in lung are activated to secrete the anti-inflammatory protein TSG-6. *Cell Stem Cell* 5(1):54–63.
27. Caplan AI, Dennis JE (2006) Mesenchymal stem cells as trophic mediators. *J Cell Biochem* 98(5):1076–1084.
28. Lin R-Z, Moreno-Luna R, Zhou B, Pu WT, Melero-Martin JM (2012) Equal modulation of endothelial cell function by four distinct tissue-specific mesenchymal stem cells. *Angiogenesis* 15(3):443–455.